Towards a corpuscular model of optical phenomena

Jin, Fengping

Chapter 2

Hanbury Brown-Twiss Experiment with Coherent Light

This chapter was previously published as
F.Jin, H. De Raedt, and K. Michielsen, Commun. Comput. Phys. **7**, 813 (2010).

2.1 Introduction

Computer simulation is widely regarded as complementary to theory and experiment [4]. Usually, the fundamental theories of physics provide the framework to formulate a mathematical model of the observed phenomenon, often in terms of differential equations. Solving these equations analytically is a task that is often prohibitive but usually it is possible to study the model by computer simulation. Experience has shown that computer simulation is a very powerful approach to study a wide variety of physical phenomena. However, recent advances in nanotechnology are paving the way to prepare, manipulate, couple and measure single microscopic systems and the interpretation of the results of such experiments requires a theory that allows us

to construct processes that describe the individual events that are being observed. Such a theory does not yet exist. Indeed, although quantum theory (QT) provides a recipe to compute the frequencies for observing events, it does not describe individual events, such as the arrival of a single electron at a particular position on the detection screen [1, 54, 65, 67]. Thus, we face the situation that we cannot rely on an established physical theory to build a simulation model for the individual processes that we observe in real experiments. Of course, we could simply use pseudo-random numbers to generate events according to the probability distribution that is obtained by solving the Schrödinger equation. However, that is not what the statement "QT does not describe individual events" means. What it means is that QT tells us nothing about the underlying processes that give rise to the frequencies of events observed after many of these events have been recorded. Therefore, in order to gain a deeper understanding in the processes that cause the observed event-based phenomena, it is necessary to model these processes on the level of individual events without using QT. The challenge therefore is to find algorithms that simulate, event-by-event, the experimental observations that, for instance, interference patterns appear only after a large number of individual events have been recorded by the detector [67, 79], without first solving the Schrödinger equation.

In this chapter, we leave the conventional line-of-thought, postulating that it is fundamentally impossible to give a logically consistent description of the experimental results in terms of causal processes of individual events. In other words, we reject the dogma that there is no explanation that goes beyond the quantum theoretical description in terms of averages over many events and search for an explanation of the experimental facts in terms of elementary, particle-like processes. It is not uncommon to find in the recent literature, statements that it is impossible to simulate quantum phenomena by classical processes. Such statements are thought to be a direct consequence of Bell's theorem [5] but are in conflict with other work that has pointed out the irrelevance of Bell's theorem [6–28, 80]. This conclusion is supported by several explicit examples that prove that it is possible to construct algorithms that satisfy Einstein's criterion for locality and causality, yet reproduce *exactly* the two-particle correlations of a quantum system in the singlet state, without invoking any concept of QT [29–34]. It is therefore an established fact that purely classical processes can produce the correlations that are characteristic for a quantum system in an entangled state, proving that from the viewpoint of simulating quantum phenomena on a digital computer, Bell's no-go theorem is of no relevance whatsoever.

The present chapter builds on earlier work [29–34, 55–61, 81] that demonstrates that quantum phenomena can be simulated on the level of individual events without first solving a wave equation or invoking concepts of QT, wave theory or probability theory. Specifically, we have demonstrated that it is possible to construct event-by-event processes, that reproduce the results of QT for single-photon beam-splitter and Mach-Zehnder interferometer experiments [79], Einstein-Podolsky-Rosen-Bohm experiments with photons [38, 82, 83], Wheeler's delayed-choice experiment with single

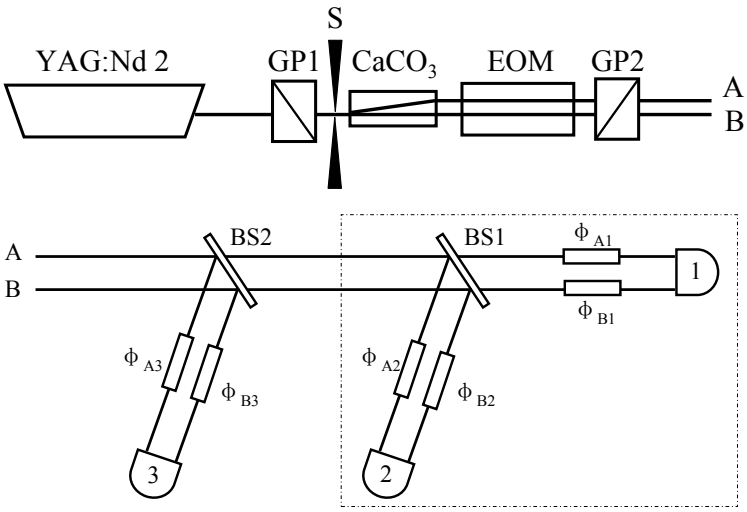

Figure 2.1: Schematic picture of a HBT experiment [36]. Top: Source. Coherent light, generated by a YAG laser, is sent through the Gan prism GP1,a single slit S, a beam splitter (a $CaCO_3$ crystal), an electro-optic modulator (EOM) and another Gan prism GP2 to produce two beams A and B as if they would have emerged from a double slit separated by 1.3 mm [36]. The EOM is switched rapidly to destroy the first-order coherence between beams A and B. Bottom: The interferometer consists of two beam splitters $BS1$ and $BS2$ and phase shifters ϕ_{An} and ϕ_{Bn} $(n = 1, 2, 3)$. Light intensity is measured by the three detectors D_1, D_2 and D_3.

photons [84], quantum eraser experiments with photons [37], double-slit and two-beam single-photon interference, quantum cryptography protocols, and universal quantum computation [57, 58]. According to the theory of quantum computation, the latter proves that at least in principle, we can construct particle-like, event-by-event processes that can simulate any quantum system [85]. Some interactive demonstration programs can be downloaded from `http://www.compphys.net` and Ref. [62].

In our earlier work, we studied first-order interference only. In this chapter, we extend the range of applications of the event-based simulation approach by demonstrating that the event-based algorithms, used in our previous work, can be re-used, without modification, to build a particle-only simulation model for another fundamental physics experiment, the Hanbury Brown-Twiss (HBT) experiment [86]. The HBT effect refers to a variety of correlation and anti-correlation effects in the intensities received by two or more detectors from a beam of particles [87–89], examples being second and third order interference. According to common lore, when a HBT experiment is performed using single-particle detectors, the HBT effect is attributed to the wave-particle duality of the beam. In this chapter, we present a particle-only model of the HBT effect, demonstrating that it is possible to construct causal, particle-like processes that describe the experimental facts without invoking concepts of QT.

As a concrete realization, we consider a recent HBT experiment [36], a schematic

picture of which is shown in Fig. 2.1. A radiation source, a frequency doubled Q-switched Nd:YAG laser with wavelength $532nm$, is used. The coherent light from this source is split by a beam splitter. The electro-optical modulator (EOM) erases the first-order interference of the light [36]. The two beams that emerge are labeled A and B, see Fig. 2.1(top). Then, the two beams are sent to three detectors through two beam splitters (BS), see Fig. 2.1(bottom). After measuring the coincidences between the signals of the three detectors by means of a triple coincidence circuit (TCC), the third-order intensity interference pattern is observed [36].

The purpose of this chapter is to demonstrate that one can construct a simulation model of this experiment that

- is a one-to-one copy of the experimental setup such that each device in the real experiment has a counterpart in the simulation algorithm
- is event-based and satisfies elementary physical (Einstein's) requirements of local causality
- reproduces the results of wave theory by means of particles only.

The structure of the chapter is as follows. In Section 2, we briefly review the wave theory of second and third-order interference. The simulation model is described in Section 3. Section 4 presents our simulation results and a discussion thereof. Our conclusions are given in Section 5.

2.2 Wave theory

Conceptually, the experiment of Fig. 2.1 can be viewed as a double-slit type experiment with three detectors, as shown in Fig. 2.2. Assume that source A emits coherent light with amplitude α and that source B emits coherent light with amplitude β. Thus, according to the superposition principle, the total amplitude falling on the n-th detector ($n = 1, 2, 3$) is

$$a_n = \alpha e^{i\phi_{An}} + \beta e^{i\phi_{Bn}}, \tag{2.1}$$

where ϕ_{An} (ϕ_{Bn}) is the accumulated phase of the photon travelling from source A (B) to the n-th detector. While the intensity is

$$I_n = |a_n|^2 = I_A + I_B + 2\mathbf{Re}\alpha\beta^* e^{i\phi_n}, \tag{2.2}$$

where $I_A = |\alpha|^2$, $I_B = |\beta|^2$, and $\phi_n = \phi_{An} - \phi_{Bn}$. If the relative phase of α and β is fixed, Eq. (2.2) predicts that interference fringes will be observed. This type of interference is referred to as first-order interference. If there is no correlation between the phases of α and β, there are no interference fringes because

$$\langle I_n \rangle = \langle I_A \rangle + \langle I_B \rangle. \tag{2.3}$$

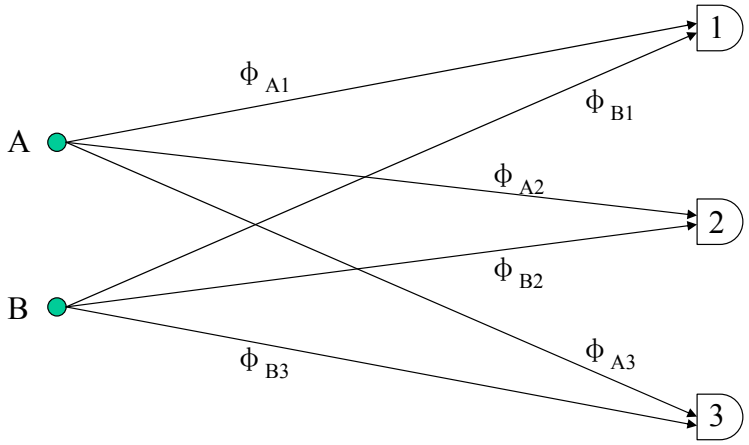

Figure 2.2: Schematic picture of third order intensity correlation. Photons emitted from sources A and B are registered by three detectors D_1, D_2 and D_3. ϕ_{An} and ϕ_{Bn} $(n = 1, 2, 3)$ are the phases accumulated during their flight from sources A or B to the n-th detector.

On the other hand, the product of the intensities is given by

$$I_n I_m = |a_n a_m|^2 = |\alpha^2 e^{i(\phi_{An}+\phi_{Am})} + \beta^2 e^{i(\phi_{Bn}+\phi_{Bm})} + \alpha\beta(e^{i(\phi_{An}+\phi_{Bm})} + e^{i(\phi_{Am}+\phi_{Bn})})|^2, \tag{2.4}$$

and after averaging over the uncorrelated phases of α and β, we find

$$\begin{aligned} G^{(2)}_{nm} &= \langle I_n I_m\rangle = \langle I_A I_A\rangle + \langle I_B I_B\rangle + \langle I_A I_B\rangle |e^{i(\phi_{An}+\phi_{Bm})} + e^{i(\phi_{Am}+\phi_{Bn})}|^2 \\ &= \langle I_A^2\rangle + \langle I_B^2\rangle + 2\langle I_A I_B\rangle(1+\cos\phi_{nm}) \end{aligned} \tag{2.5}$$

where $\phi_{nm} = \phi_n - \phi_m$ and $n, m = 1, 2, 3$. According to Eq. (2.5) the intensity-intensity correlation will exhibit interference fringes, a manifestation of the so-called Hanbury Brown-Twiss effect. This type of interference is referred to as second-order interference. It is convenient to introduce the normalized, dimensionless, correlation by

$$g^{(2)}_{nm} \equiv \frac{G^{(2)}_{nm}}{\langle I_n\rangle\langle I_m\rangle}, \tag{2.6}$$

where $\langle I_n\rangle = \langle I_m\rangle = \langle I_A\rangle + \langle I_B\rangle$. Assuming that the sources A and B have the same statistics and the same average intensities, we have $I_A = I_B$ and obtain

$$g^{(2)}_{nm} = g^{(2)}\left(1 + \frac{1}{2}\cos\phi_{nm}\right), \tag{2.7}$$

where $g^{(2)} = \langle I_A^2\rangle/\langle I_A\rangle^2$ is the second-order normalized intensity autocorrelation function. Similarly, we consider the averages of the product of three intensities given by

$$G^{(3)}_{123} = \langle I_1 I_2 I_3\rangle = \langle I_A^3\rangle + \langle I_B^3\rangle + [\langle I_A^2\rangle\langle I_B\rangle + \langle I_B^2\rangle\langle I_A\rangle][3 + 2(\cos\phi_{12} + \cos\phi_{23} + \cos\phi_{13})], \tag{2.8}$$

and, assuming $I_A = I_B$ as before, we have

$$g^{(3)}_{123} \equiv \frac{G^{(3)}_{123}}{\langle I_1\rangle\langle I_2\rangle\langle I_3\rangle} = \frac{g^{(3)}}{4} + \frac{g^{(2)}}{2}\left(\frac{3}{2} + \cos\phi_{12} + \cos\phi_{23} + \cos\phi_{13}\right), \tag{2.9}$$

where $g^{(3)} = \langle I_A^3\rangle/\langle I_A\rangle^3$ is the third-order normalized intensity autocorrelation function. This type of interference is referred to as third-order interference. In this chapter, we consider the case of coherent light only. Then we have $g^{(3)} = g^{(2)} = 1$.

2.3 Event-by-event simulation

We first discuss the general aspects of our event-by-event, particle-only simulation approach. This approach is unconventional in that it does not require knowledge of the wave amplitudes obtained by first solving the wave mechanical problem nor do we first calculate the quantum potential (which requires the solution of the Schrödinger equation) and then compute the Bohm trajectories of the particles. Instead, the detector clicks are generated event-by-event by locally causal, adaptive, classical dynamical systems. Our approach employs algorithms, that is we define processes, that contain a detailed specification of each individual event which cannot be derived from a wave theory.

The simulation algorithms define processes that are most easily viewed in terms of events, messages, and units that process these events and messages. In a pictorial description, the photon is regarded as a messenger, carrying a message that represents its time-of-flight. In this pictorial description, we may speak of "photons" generating the detection events. However, these so-called photons, as we will call them in the following, are elements of a model or theory for the real laboratory experiment only. The only experimental facts are the settings of the various apparatuses and the detection events.

The processing units mimic the role of the optical components in the experiment. A network of processing units represents the complete experimental setup. The standard processing units consist of an input stage, a transformation stage and an output stage. The input (output) stage may have several channels at (through) which messengers arrive (leave). Other processing units are simpler in the sense that the input stage is not necessary for the proper functioning of the device. A message is represented by a set of numbers, conventionally represented by a vector. As a messenger arrives at an input channel of a processing unit, the input stage updates its internal state, represented by a vector, and sends the message together with its internal state to the transformation stage that implements the operation of the particular device. Then, a new message is sent to the output stage which selects the output channel through which the messenger will leave the unit. At any given time, there is only one messenger being routed through the whole network. There is no direct communication between the messengers nor is there any communication between the processing units other

than through the messengers. We view the simulation as a message-processing and message-passing process: It routes messengers, representing the photons, through a network of message-processing units, representing the optical components in the laboratory experiment. From this general description, it should already be clear that the process that is generated by the collective of classical dynamical systems is locally causal in Einstein's sense.

2.3.1 Simulation model

The network of processing units represents the whole experimental setup. For the present purpose, that is the demonstration that the HBT effect can be explained by a particle-only model, it is sufficient to simulate the bottom part of Fig. 2.1. All the components, photons, beam splitters and photon detectors, have corresponding parts in our event-based simulation. As all the components are already presented in our previous work [29–32, 34, 55–61, 81], for completeness, we only give a brief description of each of the components of the simulation setup.

2.3.1.1 Messenger

We view each photon as a messenger. Each messenger has its own internal clock, the hand of which rotates with frequency f. When the messenger is created, the time of the clock is set to zero. As the messenger travels from one position in space to another, the clock encodes the time of flight t modulo the period $1/f$. The message, the position of the clock's hand, is most conveniently represented by a two-dimensional unit vector $\mathbf{e}_j = (e_{0,j}, e_{1,j}) = (\cos\psi_j, \sin\psi_j)$, where $\psi_j = 2\pi f t_j$ and the subscript $j > 0$ labels the successive messages. The messenger travels with the speed of light c. In this chapter, we do not need to specify the fixed frequency f and to specify a message, we use the angle ψ_j instead of the time-of-flight t_j.

2.3.1.2 Beam splitter

The structure of the processing unit for a beam splitter (BS) is shown in Fig. 2.3. The unit has two input and two output channels labeled by $k = 0, 1$ and consists of an input stage (DLM), a transformation stage (T), and an output stage (O). The input stage receives a message on either input channel 0 or 1, never on both channels simultaneously. The input events are represented by the vectors $\mathbf{v}_j = (1, 0)$ or $\mathbf{v}_j = (0, 1)$ if the jth event occurred on channel 0 or 1, respectively and are processed by a simple deterministic learning machine (DLM) [55–58, 60]. The DLM has two internal registers $\mathbf{Y}_{k,j} = (C_{k,j}, S_{k,j})$ and one internal vector $\mathbf{x}_j = (x_{0,j}, x_{1,j})$, where $x_{0,j} + x_{1,j} = 1$ and $x_{k,j} \geq 0$ for $k = 0, 1$ and all $j > 0$. Upon receiving the jth input event, the DLM performs the following steps: It stores the input message $\mathbf{e}_{k,j} = (\cos\psi_{k,j}, \sin\psi_{k,j})$ in its internal register $\mathbf{Y}_{k,j} = (C_{k,j}, S_{k,j})$. Then, it updates

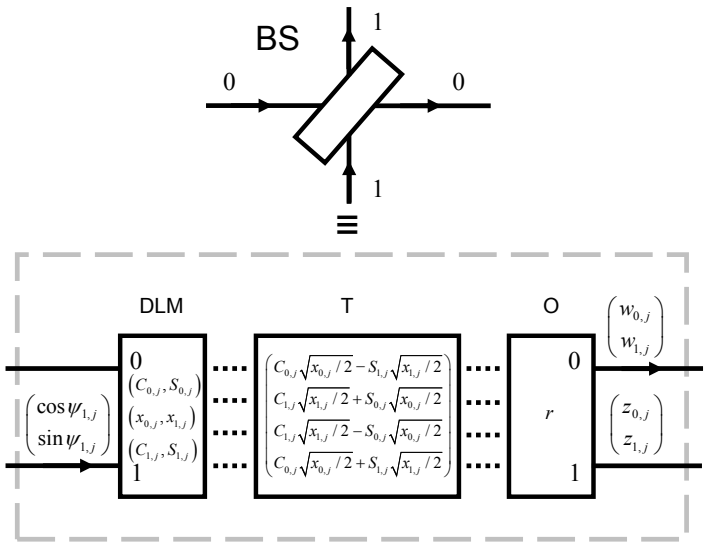

Figure 2.3: Diagram of a DLM-based processing unit that performs an event-based simulation of a beam splitter (BS). The processing unit consists of three stages: An input stage (DLM), a transformation stage (T) and an output stage (O). The solid lines represent the input and output channels of the BS. The dotted lines indicate the data flow within the BS.

its internal vector according to the rule

$$\mathbf{x}_j = \gamma \mathbf{x}_{j-1} + (1-\gamma)\mathbf{v}_j \ , \tag{2.10}$$

where $0 < \gamma < 1$. A detailed analysis of the update rule Eq. (2.10) can be found in Ref. [81].

The transformation stage accepts the messages from the input stage, and transforms them into a new four-dimensional vector

$$\mathbf{T} = \frac{1}{\sqrt{2}} \begin{pmatrix} C_{0,j}\sqrt{x_{0,j}} - S_{1,j}\sqrt{x_{1,j}} \\ C_{1,j}\sqrt{x_{1,j}} + S_{0,j}\sqrt{x_{0,j}} \\ C_{1,j}\sqrt{x_{1,j}} - S_{0,j}\sqrt{x_{0,j}} \\ C_{0,j}\sqrt{x_{0,j}} + S_{1,j}\sqrt{x_{1,j}} \end{pmatrix} . \tag{2.11}$$

The output stage sends out a messenger (representing a photon) carrying the message

$$\mathbf{w} = \begin{pmatrix} w_{0,j} \\ w_{1,j} \end{pmatrix} , \tag{2.12}$$

where

$$w_{0,j} \quad = \quad \left(C_{0,j}\sqrt{x_{0,j}/2} - S_{1,j}\sqrt{x_{1,j}/2} \right) \Big/ \, s_j \ ,$$

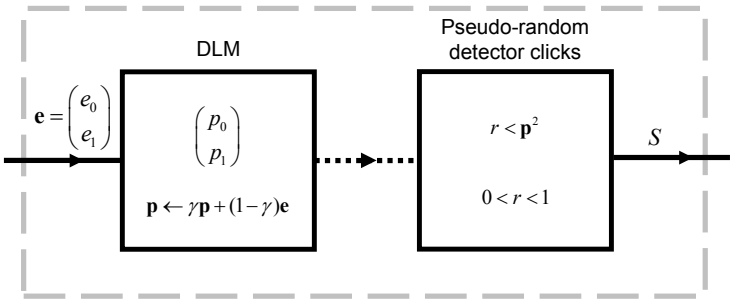

Figure 2.4: Diagram of the event-based detector model defined by Eqs. (2.16) and (2.17). The dotted line indicates the data flow within the processing unit.

$$\begin{aligned} w_{1,j} &= \left(C_{1,j}\sqrt{x_{1,j}/2} + S_{0,j}\sqrt{x_{0,j}/2}\right) \Big/ s_j \ , \\ s_j &= \sqrt{w_{0,j}^2 + w_{1,j}^2}. \end{aligned} \tag{2.13}$$

through output channel 0 if $s_j^2 > r$ where $0 < r < 1$ is a uniform pseudo-random number. Otherwise, if $s_j^2 \leq r$, the output stage sends through output channel 1 the message

$$\mathbf{z} = \begin{pmatrix} z_{0,j} \\ z_{1,j} \end{pmatrix}, \tag{2.14}$$

where

$$\begin{aligned} z_{0,j} &= \left(C_{1,j}\sqrt{x_{1,j}/2} - S_{0,j}\sqrt{x_{0,j}/2}\right) \Big/ t_j \ , \\ z_{1,j} &= \left(C_{0,j}\sqrt{x_{0,j}/2} + S_{1,j}\sqrt{x_{1,j}/2}\right) \Big/ t_j \ , \\ t_j &= \sqrt{z_{0,j}^2 + z_{1,j}^2}. \end{aligned} \tag{2.15}$$

We use pseudo-random numbers to mimic the apparent unpredictability of the experimental data only: The use of pseudo-random numbers to select the output channel is not essential [56]. Note that in our simulation model there is no need to introduce the (quantum theoretical) concept of a vacuum field, a requirement in the quantum optical description of a BS.

2.3.1.3 Photon detector

A schematic diagram of the unit that functions as a single-photon detector is shown in Fig. 2.4 [81]. The first stage consists of a DLM that receives on its input channel the jth message represented by the two-dimensional vector $\mathbf{e}_j = (\cos\psi_j, \sin\psi_j)$. In this chapter, we use the simplest DLM containing a single two-dimensional internal vector with Euclidean norm less or equal than one.

We write $\mathbf{p}_j = (p_{0,j}, p_{1,j})$ to denote the value of this vector after the jth message has been received. Upon receipt of the jth message the internal vector is updated according to the rule

$$\mathbf{p}_j = \gamma \mathbf{p}_{j-1} + (1-\gamma)\mathbf{e}_j \ , \tag{2.16}$$

where $0 < \gamma < 1$ and $j > 0$. A machine that operates according to the update rule Eq. (2.16) has memory to store an amount of information that is equivalent to the information carried by a single message only. Obviously, the rule Eq. (2.16) is the same as that used for the BS (see Eq. (2.10)) but the input data is different.

The second stage of the detector (see Fig. 2.4) uses the information stored in the internal vector to decide whether or not to generate a click. As a highly simplified model for the bistable character of the real photodetector or photographic plate, we let the machine generate a binary output signal S_j using the threshold function

$$S_j = \Theta(\mathbf{p}_j^2 - r_j), \tag{2.17}$$

where $\Theta(.)$ is the unit step function and $0 \leq r_j < 1$ is a uniform pseudo-random number. Note that in contrast to experiment, in a simulation, we could register both the $S_j = 0$ and $S_j = 1$ events such that the number of input messages equals the sum of the $S_j = 0$ and $S_j = 1$ detection events. Since in experiment it cannot be known whether a photon has gone undetected, we discard the information about the $S_j = 0$ detection events in our future analysis. The total detector count is defined as

$$N = \sum_{j=1}^{N_R} S_j \ , \tag{2.18}$$

where N_R is the number of messages received. Thus, N counts the number of one's generated by the machine.

2.3.1.4 Experiment

The processing units that simulate the optical components are connected in such a way that the network corresponds to the experimental setup in the laboratory. As explained earlier, it is sufficient to consider the bottom part of Fig. 2.1.

2.4 Simulation results

Our aim is to show that the event-based simulation model is capable of reproducing the wave mechanical results of the laboratory experiment [36] schematically shown in Fig. 2.1. As these laboratory experiments are carried out with continuous light and do not probe the individual photon regime, we cannot expect to see effects that relate to individual light quanta. Hence we expect that the results agree with those derived from classical electrodynamics. Accordingly, in this chapter we take the time

window that defines the coincidences large enough such that there are no quantum correlations. For a more extensive discussion of this important point, see Section 2.4.4.

Following Ref. [36], the phase of the coherent photons emitted by the source is "randomized" by letting the light pass through an EOM, the voltage of which is switched with a frequency of 50 Hz. To mimic this in the simulation, we send $N_{interval}$ messengers with some fixed but randomly chosen phase, then another $N_{interval}$ messengers with another fixed but randomly chosen phase, and so on. In practice, we use $N_{interval} = 2500$. The messengers (photons) are sent through either channel A or B, one at a time and are either transmitted or reflected by the beam splitters. Before hitting a detector, the messenger experiences a time delay corresponding to ϕ_{An} or ϕ_{Bn} $(n = 1, 2, 3)$. The detector processes the message carried by the messenger and decides whether or not to produce a click.

We consider three different experiments. In case 1, we remove both BSs in Fig. 2.1 (bottom) and study the signal produced by detector D_1. Then, in case 2, we remove BS2, that is we consider the HBT experiment with two detectors, as indicated by the dashed-dotted line in Fig. 2.1 (bottom). Finally, in case 3, we study the full three-photon correlation experiment, see Fig. 2.1 (bottom). In cases 2 (3), the intensity-intensity correlations are calculated by counting coincidences of two (three) messengers, meaning that the arrival times of the two (three) messengers are within a time window W, to be discussed in Section 4.4. All simulations have been carried out with $\gamma = 0.99$.

2.4.1 Case 1: One detector

Let us first demonstrate how the event-based model of the detector works [81]. To this end, we remove BS1 and BS2 in Fig. 2.1 (bottom). The messengers, randomly entering through channels A or B, are sent directly to the time-delay units that change the angle of the hand of the clock representing the time-of-flight by ϕ_{A1} or ϕ_{B1}, respectively. The messengers are then processed by detector D_1. We perform two different sets of simulations. First, we keep the differences between the time-of-flights of the messengers entering channel A and the time-of-flights of the messengers entering channel B constant. In this case, according to wave theory, we expect to see clear interference fringes. Second, the differences between the time-of-flights of the messengers entering channel A and the time-of-flights of the messengers entering channel B are taken to be random. Then, according to wave theory, there should be no sign of interference effects. Hence, as shown in Fig. 2.5, our particle-only simulation approach reproduces both features and the results are in very good agreement with the wave theoretical results (see Eq. (2.2)).

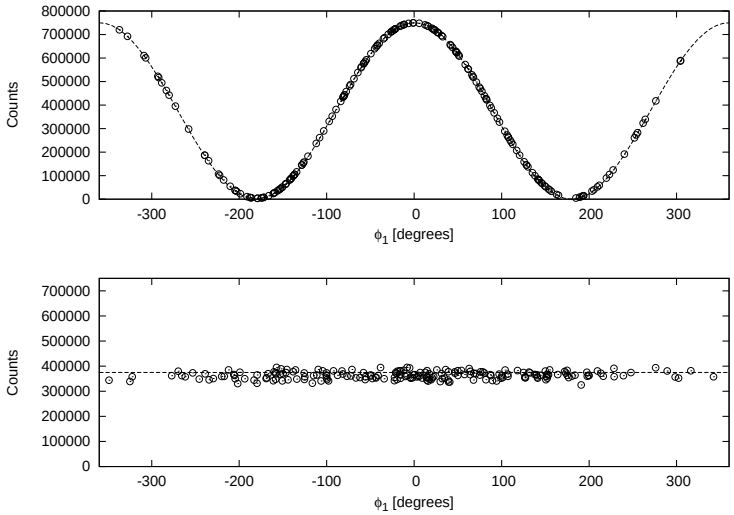

Figure 2.5: Case 1: All BSs in Fig. 2.1 (bottom) removed. Simulation results for the detector counts as a function of $\phi_1 = \phi_{A1} - \phi_{B1}$. The differences between the time-of-flights of the messengers entering channel A and the time-of-flights of the messengers entering channel B are constant (top) or random (bottom, see text). Circles: Simulation data; Dashed line: Wave theoretical solution Eq. (2.2) (top) and Eq. (2.2) averaged over ϕ_1 (bottom).

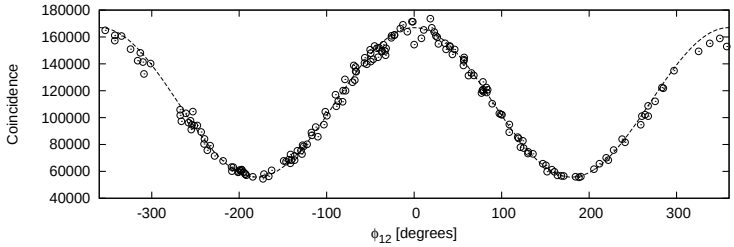

Figure 2.6: Case 2: BS2 in Fig. 2.1 (bottom) removed. Simulation results of the two-particle coincidence counts as a function of ϕ_{12} where $\phi_{12} = \phi_1 - \phi_2$, and $\phi_n = \phi_{An} - \phi_{Bn}$ $(n = 1, 2)$. The time-of-flights of the messengers entering channel A and the time-of-flights of the messengers entering channel B are taken to be random (see text). Circles: Simulation data; Dashed line: Wave theoretical solution Eq. (2.7).

2.4.2 Case 2: Hanbury Brown-Twiss experiment

We consider the HBT experiment with two detectors, that is we remove BS2 from the diagram in Fig. 2.1 (bottom). Messengers enter the apparatus through channel A or B, one by one. The time-of-flights of the messengers entering channel A and the time-of-flights of the messengers entering channel B are taken to be random. Hence, as shown in Fig. 2.5 (bottom) there is no first-order interference. When passing a BS,

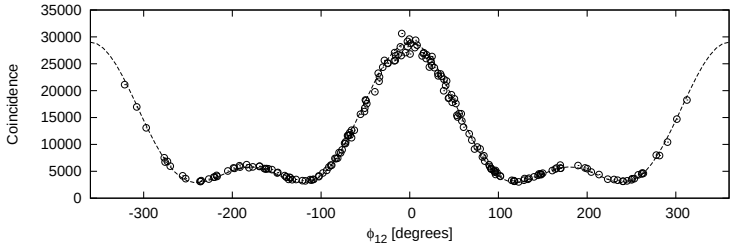

Figure 2.7: Case 3: Three particle correlation experiment (see Fig. 2.1 (bottom)). Simulation results of the three-particle coincidence counts as a function of ϕ_{12} where $\phi_{12} = \phi_1 - \phi_2$, and $\phi_n = \phi_{An} - \phi_{Bn}$ $(n = 1, 2, 3)$. We only show data for the case $\phi_{A2} = \phi_{B2} = 0$, $\phi_{A1} = \phi_{B3}$, $\phi_{B1} = \phi_{A3}$ where ϕ_{A1} and ϕ_{B1} are chosen randomly. The time-of-flights of the messengers entering channel A and the time-of-flights of the messengers entering channel B are taken to be random (see text). Circles: Simulation data; Dashed line: Wave theoretical solution Eq. (2.9).

the message changes according to the rules explained in Section 2.3.1.2. Then, before entering the detector, the message is changed once more by ϕ_{An} or ϕ_{Bn} $(n = 1, 2)$, depending on which path the messenger took. If the two detectors fire with the time window W (see Section 4.4), we increase the number of coincidences. The simulation data shown in Fig. 2.6 confirm that this procedure reproduces the results of wave theory, see Eq. (2.7).

2.4.3 Case 3: Three-particle intensity-intensity correlation

Finally, we consider the laboratory experiment [36] that measures the correlations between three detectors (see Fig. 2.1). The simulation procedure is the same as in case 2, except that we count coincidences of clicks of three different detectors. Also in this case, the simulation data shown in Fig. 2.7 confirm that this procedure reproduces the results of wave theory, see Eq. (2.9).

2.4.4 Discussion

Our simulation model is based on a particle picture and makes no reference to concepts or results from wave theory. In contrast to the conventional quantum theoretical explanation in terms of the wave-particle nature of photons, our simulation approach requires a particle picture of photons only. During the event-by-event simulation we always have full which-way information of the photons (messengers) since we can always track them. Nevertheless, depending on the settings of the optical apparatuses, intensity-intensity interference is observed. Although the appearance of an interference pattern is commonly considered to be characteristic of a wave, we have demonstrated that, as in experiment, it can also appear as a result of a collection of

particles that interact with the various optically active devices such as beam splitters and detectors.

It is of interest to ask what aspects of the model are essential for producing the correct interference patterns. There are three different aspects that need to mentioned, namely (1) the discrete-event nature of the simulation, (2) the memory in both the beam splitter and detector model and (3) the threshold feature of the detector model.

Obviously, as our model is event-based, the simulation proceeds in discrete "time steps". It has been shown [90] that Newton's equation in a discretized form with a finite time-step can also produce interference patterns (although it is not clear yet whether this approach can reproduce the results that derive from Maxwell's theory). However, in our approach the discrete time label j plays a very different role from that of the discrete time step in discretized classical equations of motion. The label j merely serves to label successive events and does not have the dimension of time. In our idealized model, it does not matter how far, in real time, successive events are separated from each other. To make our model more realistic, we could introduce a "real time" by specifying how many events per unit of time are being processed. As it is the aim of this chapter to demonstrate that the same processing units as those used for very different purposes can, without making any modification, be combined to reproduce the results of HBT experiments (as described by Maxwell's theory), the simulations are performed such that the event-based system operates in its stationary regime, corresponding to the regime in which the number of events per time unit is large.

In our approach, interference appears as a result of processing individual events. Clearly, under these circumstances it is impossible to explain in a logical, rational manner the appearance of interference without some form of indirect communication between individual events. In our models, the local memory in the DLMs together with the update rules (see Sec. 2.3.1.2 and 2.3.1.3) provide the mechanism for this indirect communication to take place. In the HBT experiments that we simulate in the present chapter, only the memory in the detector is essential. For other types of experiments [55–57, 60, 61], also the memory in the beam splitter is essential. The detector model (which does not rely on concepts of probability theory) that we employ is very different from models that are based on the hypothesis that memory effects in the equipment, operating as a random dynamical system over the field of p-adic numbers, can lead to interference phenomena [91, 92].

Regarding the threshold mechanism, it is intuitively clear that single-photon detectors must necessarily operate as a threshold device because they have to discriminate between no and one photon. The presence of a threshold may have far reaching implications. For instance, it has been shown that it may lead to apparent violations of the Bell inequalities observed in EPRB experiments with photons [93]. The detector model employed in this chapter differs from models discussed in Ref. [93] in that there is a simple, one-to-one relation between the equations describing the event-based model and the material equations in Maxwell's theory [81].

Finally, we address the question of simulating quantum correlations (changing the factor of 1/2 in Eq. (2.7) into one) in HBT experiments. In real experiments, and also in our simulation approach, it is necessary to specify the procedure by which we count coincidences of detection events. For the experiments at hand, one introduces a time window W and one defines as a two (three) particle coincidence, two (three) detection events with the time difference(s) are smaller than W. As discussed extensively in our work on the simulation of Einstein-Podolsky-Rosen-Bohm (EPRB) experiments [29], the choice of the time window W is of crucial importance, both in the simulation and in real experiments [38], to obtain the correlation of a quantum system in the singlet state. In general, only when $W \to 0$, experiment and simulation can reproduce the correlation of a quantum system in the singlet state [29]. For large enough W, the relation to a quantum system in the singlet state is lost. In this chapter, we have chosen W sufficiently large and generated groups of two (three) messengers such that if the two (three) detectors fire, this constitutes a coincidence of two (three) particles. In other words, the time delays are only used by the detector but are ignored in determining coincidences. In this sense, the simulation results presented in this chapter pertain to classical light and are therefore in excellent agreement with classical wave theory. To study the quantum aspects of two- and three-particle correlations the time delays should be used to also determine the coincidences, as in our EPRB simulations [29]. For completeness we mention that in this chapter, we considered light sources that produces photons in a coherent state only. We leave the study of quantum and thermal features in these correlation experiments for future research.

2.5 Conclusion

We have demonstrated that our classical, locally causal, particle-like simulation approach reproduces the results of the Hanbury Brown-Twiss effect. Our event-based simulation model, a classical, locally causal, adaptive dynamical system, reproduces the results of wave theory without making reference to the solution of a wave equation and provides a simple, particle-based mental picture for what each individual photon experiences as it travels from the source to the detector. Our simulation algorithm demonstrates that the wave-particle duality is not the only way to describe the nature of a photon but that there is another way that only needs the particle nature, satisfies Einstein's local causality and does not defy the common sense. Finally, we would like to emphasize that the algorithms used to simulate the optical components in this chapter have not been designed to simulate the HBT-type experiments. The algorithms have been taken, without modification, from our earlier work on very different quantum optics experiments [29–32, 34, 55–61, 81, 81]. In this sense, it seems that our approach has predictive power: The algorithms can be reused to simulate very different experiments than those for which they were originally developed.

Finally, we would like to draw attention to the fact that our event-based simulation

models make specific predictions that can be tested in properly designed experiments. First, we recall that the distribution that the simulation model produces when it has reached the stationary regime agrees with wave theory and will therefore be in concert with any experiment that reproduces the results of wave theory. However, we can also simulate the system in the transient regime in which the convergence to the correct, stationary distribution can be monitored. Our simulation models make specific predictions for the transient behavior of the distribution of events because they depend on the details of the model [81]. Thus, a meaningful confrontation of our model with experiment requires that the latter has recorded all the events, starting with the very first photon that is detected (and not after alignment, calibration etc. has been performed). We hope that our work creates a stimulus to carry out such experiments.